

See discussions, stats, and author profiles for this publication at: <https://www.researchgate.net/publication/231630823>

Interpretation of XPS O (1s) in Mixed Oxides Proved on Mixed Perovskite Crystals

ARTICLE *in* THE JOURNAL OF PHYSICAL CHEMISTRY B · DECEMBER 2001

Impact Factor: 3.3 · DOI: 10.1021/jp012040a

CITATIONS

49

READS

74

5 AUTHORS, INCLUDING:



Dorota A. Pawlak

Institute of Electronic Materials Technology

91 PUBLICATIONS **785** CITATIONS

SEE PROFILE



Kiyoshi Shimamura

National Institute for Materials Science

136 PUBLICATIONS **1,798** CITATIONS

SEE PROFILE

Interpretation of XPS O (1s) in Mixed Oxides Proved on Mixed Perovskite Crystals

Dorota A. Pawlak,^{*,†} Masahiko Ito, Masaaki Oku, Kiyoshi Shimamura, and Tsuguo Fukuda

Institute for Materials Research, Tohoku University, Sendai, 980-8577 Japan

Received: May 30, 2001; In Final Form: October 26, 2001

Mixed perovskites $(AA')(BB')O_3$, where $A = \text{La}$ or Nd , $A' = \text{Sr}$, $B = \text{Al}$ or Ga , and $B' = \text{Ta}$ or Nb , were investigated by X-ray photoelectron spectroscopy (XPS). The interpretation of XPS O(1s) signals in mixed oxides is discussed. The nonsingular O(1s) peak that occurs in the mixed oxides is due to the polarization of the oxygen valence electron density, as was already proposed by us for $\text{Y}_3\text{Al}_5\text{O}_{12}$ and YAlO_3 . This interpretation seems to be true also for the case when four different metals are in the oxide. The O(1s) binding energies seem to depend on the direction in which they are ejected.

Introduction

X-ray photoelectron spectroscopy, XPS, got the name electron spectroscopy for chemical analysis, ESCA, after Kai Siegbahn and his group found that this spectroscopy produces chemical shifts.^{1,2} Electrons of the same energy level of particular elements, e.g., Al(2p), located in different environments are observed at different binding energies.

In this work, we discuss the model of interpreting the O(1s) XPS signals in mixed oxides. There are not many reports giving detailed O(1s) data, because the interpretation is not clear. Citing Barr³ "... many ESCA scientists fail to report any O(1s) results when examining complex oxides ...". There are only a few data: the binding energies for silicas, zeolites, and aluminates are given in refs 4–9. The interpretations of the BE shifts of the O(1s) photoelectron lines of zeolites are controversial.

It has been noticed that the O(1s) oxygen signal in mixed oxides has a complicated, nonsingular shape. The splitting of the O(1s) oxygen peak was reported for compounds with the garnet structure $\text{Y}_3\text{Al}_5\text{O}_{12}$ ¹⁰ and $\text{RE}_3\text{Fe}_5\text{O}_{12}$,¹¹ where $\text{RE} = \text{Eu}$ or Dy , and compounds with the perovskite structure YAlO_3 ¹² and REFeO_3 ,¹¹ where $\text{RE} = \text{Dy}$, Ho , or Er . In ref 10, we discuss our model, which allows for the interpreting the O(1s) signals in mixed oxides. This was discussed for mixed oxides with two different cations. In this paper, we show that this model also works when there are more than two cations in the oxide. That is why in this work we investigated mixed perovskites $(AA')(BB')O_3$, where $A = \text{La}$ or Nd , $A' = \text{Sr}$, $B = \text{Al}$ or Ga , and $B' = \text{Ta}$ or Nb . We also suggest that our model should work for any other anion or cation, which in the first shell is surrounded by atoms of different kinds. In the future, we plan to check it for fluorides.

Experimental Procedure

Crystal Growth. Four different single crystals with the composition, $(AA')(BB')O_3$, where $A = \text{La}$ or Nd , $A' = \text{Sr}$, $B = \text{Al}$ or Ga , and $B' = \text{Ta}$ or Nb , were obtained. All crystals were grown using the Czochralski method.¹³ The melts were prepared from high purity oxides (99.99%) with the composi-

tions $\text{La}_{0.30}\text{Sr}_{0.70}\text{Al}_{0.65}\text{Ta}_{0.35}\text{O}_3$ (LSAT), $\text{Nd}_{0.40}\text{Sr}_{0.60}\text{Al}_{0.70}\text{Ta}_{0.30}\text{O}_3$ (NSAT), $\text{Nd}_{0.15}\text{Sr}_{0.85}\text{Al}_{0.575}\text{Nb}_{0.425}\text{O}_3$ (NSAN), and $\text{La}_{0.15}\text{Sr}_{0.85}\text{Ga}_{0.575}\text{Nb}_{0.425}\text{O}_3$ (LSGN). The single crystals were grown from iridium crucibles, under argon atmosphere. All crystals not containing neodymium exhibited a yellowish/brownish coloration. To remove the color, the "as grown" crystals were annealed in a 0.2% H_2/Ar atmosphere at 1000 °C for 20 h. The exact description of the crystal growth process is presented elsewhere.¹⁴

X-ray Photoelectron Spectroscopy (XPS). ESCA spectra were recorded on a Surface Science Instruments ES100 spectrometer with a high-resolution X-ray monochromator. A conventional Al $K\alpha$ anode was used as a source of X-ray radiation. The background pressure during analysis was ca. 1×10^{-9} Torr. The full width at half-maximum of Au ($4f_{7/2}$) was 1.28 eV. The materials under study are insulators, producing distinctive charging shifts. These were removed using an electron flood gun and nickel net to distribute the charge homogeneously. As a reference, we used the C(1s) signal of the hydrocarbon part of the adventitious carbon (carbon of any surface adsorbed), which we fixed at 284.6 eV. This procedure has been successfully applied in a number of previous similar studies.^{3,4,10,12} Broad survey scans with a scan range from 0 to 1100 eV were run to identify all elements present in the samples, and then detailed scans (ca 20 eV wide) were recorded on which peak fitting was performed to establish precise elemental peak locations. Before measuring, all of the samples were well polished and cleaned with alcohol.

To increase the signal/noise ratio, the acquisition time for each spectrum was around 27 min. In such a case, systematic, not random, errors dominate for the spectrum.¹⁵ In our case, the intensities of the signals were very similar to each other from all four samples. Systematic errors are nearly equal in all of the investigated samples.

Results and Discussion

Four different mixed perovskite crystals $(AA')(BB')O_3$, where $A = \text{La}$ or Nd , $A' = \text{Sr}$, $B = \text{Al}$ or Ga , and $B' = \text{Ta}$ or Nb (LSAT, NSAT, LSGN, and NSAN) were investigated by XPS. A and B sites are statistically occupied by two different cations. The XPS data for the cations are given elsewhere.¹⁶ To understand how we should interpret the O(1s) data, we should analyze what is going on with the oxygen ion in mixed oxides.

* To whom correspondence should be addressed. E-mail: dora@imr.tohoku.ac.jp.

† Permanent address: Institute of Electronic Materials Technology, ul. Wolczynska 133, 01-919 Poland. E-mail: dora@alfa.chem.uw.edu.pl.

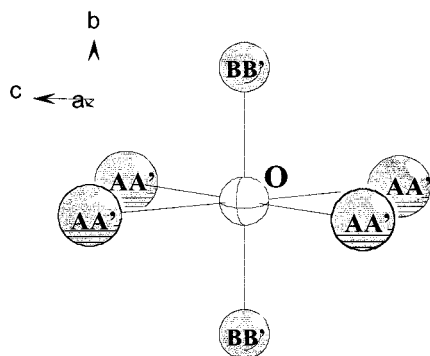


Figure 1. First coordination shell of the oxygen ion in the mixed perovskite crystals $(AA')(BB')O_3$.

Very often, the oxygen ion is approximated as having a fixed spherical size, but this is an approximation. In reality, when an oxygen ion is placed between covalent cations, its valence electronic shell is no longer uniform but polarized.³ The oxygen valence density is then oriented toward the more covalent atom. Because the bond has a covalent character, the electrons are shared with the cation. When the cations are ionic, the opposite situation holds; that is, electrons are held closer to the oxygen ion (more ionic bond). In the case of investigated mixed perovskites, the oxygen ion is placed in some kind of octahedron, between four A sites and two B sites (see Figure 1, the structures are presented elsewhere¹⁷). Both A and B sites can be statistically occupied by two different cations, A or A' and B or B'. This creates the polarization of the oxygen electron valence shell, which reflects the local perovskite structure and the composition around the oxygen.

Cations used in investigated crystals showed significant differences in the ionicity/covalency. Barr³ provides a classification of oxides, considering their ionic/covalent character. He distinguishes three different oxide types: semicovalent oxide (SCO) with the BE range of 530.5–533.0 eV, normal ionic oxide (NIO) with the BE range of 530.0 ± 0.4 eV, and very ionic oxide (VIO) with the BE range of 528.0–529.5 eV. From this, it seems that we have introduced cations belonging to the following groups: SCO (Al or Ga) and VIO (Nb, Sr, Ta, Nd, or La). The valence electron density of oxygen will be moved toward the aluminum and gallium, whereas lanthanum, neodymium, tantalum, and niobium should have the opposite effect of the electron density being closer to the oxygen ion. In more covalent bonds, e.g., Al–O and Ga–O, it will be more difficult to eject the electron, so the XPS signal will be observed at higher BE. Although in more ionic bonds, e.g., La–O, Nd–O, Ta–O, Sr–O, and Nb–O, because the electron density is closer to the oxygen ion, it will be easier to eject an electron from the oxygen; therefore, the signal will be observed at lower binding energies. Then, following the model presented before,^{10,12} the O(1s) peak should have four lines. For example, in the case of LSAT, they originate from La–O, Sr–O, Al–O, and Ta–O.

In Figure 2, the XPS O(1s) signals are shown for all four crystals. The peak fittings are done with an assumption that O(1s) has four peaks, as described above. The gray line is the experimental line, and it is overlapped by the black line, which is the fitted line. Peak positions, widths, and intensities were determined from least-squares fitting using the standard SSI software (M-Probe ESCA Software). Shirley background subtraction was used. The peak shapes were Gaussian/Lorentzian with no asymmetry. Peak fitting of the O(1s) peak into four signals was giving a good fit to the experimental total peak. In Table 1 part A, the binding energies for the O(1s) signals are

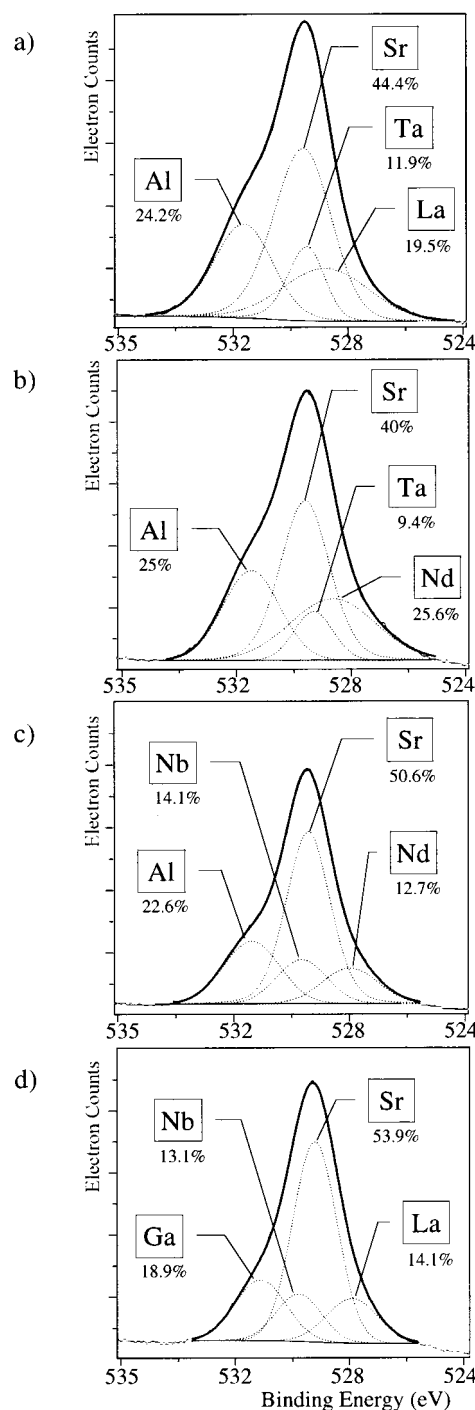


Figure 2. XPS O(1s) peaks of mixed perovskite crystals: (a) LSAT, (b) NSAT, (c) LSGN, and (d) NSAN. The total peaks are divided into four signals. The sum of these signals well fits the experimental total peak. The gray line corresponds to the experimental line, and the black corresponds to the fitted line. The callouts indicate the metal, where the simple oxide shows a similar BE to the BE of the signal on this figure, Table 1. The percentage indicates the intensity of the signals.

given. They are compared with BEs for simple oxides (bottom of Table 1 part A). It can be easily noticed that the O(1s) signals of the mixed perovskites have similar, within certain limits, binding energies to XPS O(1s) signals of simple oxides. The same effect has been observed before for other kinds of mixed oxides: $Y_3Al_5O_{12}$ and $YAlO_3$.^{10,12} This indicates that the energy of 1s electron of oxygen is distributed; that is, the energy seems to depend on the direction in which the electron is ejected from the core orbital. If it is in the direction of aluminum, then its

TABLE 1: (A) Binding Energies (BE) and (B) Full Widths at Half Maximum (FWHM) of Four Singular Peaks O(1s) for LSAT, NSAT, NSAN, LSGN, after Annealing in Reducing Atmospheres^a

A								
O(1s) binding energies [eV]								
LSAT	531.7		529.6	529.5			528.8	
NSAT	531.5		529.6	529.3	528.6			
NSAN	531.4		529.7	529.5	528.0			
LSGN		531.4	530.0	529.4				528.1
Ref. BE of O(1s) in simple oxides	531.6 ³	531.4 ³	529.6 ²⁰	530.2 ²³	529.8 ²⁰	529.3 ²⁵	528.4 ²⁶	
		531.1 ¹⁹	530.2 ²¹	530.3 ²⁴	529.9 ¹⁹	530.3 ¹⁹	528.8 ³	
			530.6 ²²				529.9 ²⁵	
simple oxides	Al ₂ O ₃	Ga ₂ O ₃	Nb ₂ O ₅	SrO	Ta ₂ O ₅	Nd ₂ O ₃	La ₂ O ₃	
<div style="display: flex; justify-content: space-around; align-items: center;"> ← SCO VIO → </div>								
B								
O(1s) fwhm [eV]								
LSAT	2.4			2.4	1.5			3.5
NSAT	2.3			2.0	1.6		3.5	
NSAN	2.3		2.0	1.8		2.3		
LSGN		2.1	1.9	1.8		-		2.1
simple oxides	Al ₂ O ₃	Ga ₂ O ₃	Nb ₂ O ₅	SrO	Ta ₂ O ₅	Nd ₂ O ₃	La ₂ O ₃	
<div style="display: flex; justify-content: space-around; align-items: center;"> ← SCO VIO → </div>								

^a The reference data for O(1s) BE of simple oxides is given in such a way as to show the similarities between the BE of simple oxides and of singular O(1s) peaks for investigated crystals.

TABLE 2: Cation Concentrations in the Investigated Crystals and Intensities of Singular Peaks of O(1s) Oxygen Signals^a

crystals	A site			B site			
	La	Nd	Sr	Al	Ga	Ta	Nb
LSAT	C ₀	0.30	0.70	0.65		0.35	
	C _S	0.29	0.72	0.64		0.36	
	I	14.5%	35.8%	31.8%		17.9%	
	I _S	19.3%	47.6%	21.2%		11.9%	
NSAT	C ₀		0.40	0.70		0.30	
	C _S		0.39	0.61	0.72	0.29	
	I	19.4%	30.4%	35.8%		14.4%	
	I _S	25.9%	40.6%	23.9%		9.6%	
NSAN	C ₀		0.15	0.85	0.575		0.425
	C _S		0.15	0.83	0.60		0.42
	I	7.5%	41.5%	30.0%			21.0%
	I _S	10.1%	55.7%	20.1%			14.1%
LSGN	C ₀	0.15		0.85	0.575		0.425
	C _S	0.12		0.88	0.56		0.44
	I	6%		44%	28%		22%
	I _S	8%		58.7%	18.6%		14.7%

^a C₀, concentration in starting raw materials; C_S, concentration in grown crystals; I, intensity of particular signals with the BE close to the binding energy of some simple oxide, which we should observe, calculated from the C_S; I_S, recalculated intensity of particular signals with the BE close to the binding energy of simple oxides, after including the local symmetry around O(1s). I_S is calculated using eq 1, where I_A and I_B correspond to the intensity of particular signals with the BE close to the binding energy of a simple oxide of A or B atoms, respectively. I_{S(A)} corresponds to I_S for A atom. Equation 1: $I_{S(A)} = (2I_A \times 100\%) / (2I_A + I_B + I_B)$.

energy is higher, that those in the direction of more ionic species, like La, Sr, etc. Each peak can be assigned to have energy similar, in some range, to O(1s) electrons of simple oxides (see Figure 2). If our interpretation is correct, the intensities of the particular peaks (Figure 2) should be comparable with the concentration of adequate cations in the crystal (I, Table 2). However, it can be noticed that they are different. The reason

for this is that we did not take into account, until now, the symmetry around the oxygen of interest. It seems that we should compare the intensities of the particular signals with the probabilities of ejecting the electron in the directions of particular cations. To calculate the probability, we need to take into account both concentration and symmetry. The core shell oxygen O(1s) electrons are spherically distributed, and photons of sufficient energy entering this shell will eject the electrons uniformly in all directions. When we consider the local symmetry and composition around the oxygen ion, then, from Figure 1, it can be seen that with good approximation it is twice as probable that the electron will be ejected in the direction of the A cation rather than the B ones. If we take this into account, then the calculated probability, I_S in Table 2, quite well agrees with the intensities of the signals presented in Figure 2. Our predictions are confirmed. We can conclude that in such a way we can interpret the XPS O(1s) data in mixed oxides. We postulate also that the same effect of directional dependence of the BE of the ejected electron should be observed for any anion or cation, which would be in the first coordination shell of different kinds of atoms, although the mechanism of such behavior is not clear. Klinowski and Barr gave the evidence that XPS signals of cations are sensitive to the second coordination shell of cations also, though not directly.¹⁸ They have shown it for aluminosilicates.

In Table 1 part B the full widths at half-maxima (fwhm) are given. The effect of decreasing binding energies (increasing ionicity of the M–O bond) is observed, as in ref 12. It can be seen both in the rows (from left to right) and in the columns of Table 1 (from top to bottom). The O(1s) signals that we associate with lanthanide ions (Nd–O and La–O) do not keep this rule. Considering the BEs of particular O(1s) signals, we can conclude that LSAT is the most covalent and LSGN the most ionic of the investigated in this paper compounds.

It is described by Barr³ that the O(1s) signal in complex oxide (formed of more ionic oxide, A_mO_n, and more covalent oxide, M_xO_y) is not as covalent or as ionic as in the two simple oxides of which it is made. In contradiction to the metal ions, which in complex oxide become more ionic (if they were already more ionic, A–O) or more covalent (if they were covalent, M–O; page 21 of ref 3). Also it is told³ that in the complex oxide "...the negative O(1s) shifts experienced by the relatively covalent M_xO_y seem to be larger than the corresponding positive shifts in the O (1s) for A_mO_n".

Actually, after the peak fitting and analyzing each O(1s) line separately, we see in our results a different situation. The O(1s) signals are behaving here not like Barr described, but they behave in the same way as the metal ions. This means in the complex oxide the oxygen O(1s) "connected" with more ionic metal will become even more ionic, and the oxygen connected with the more covalent metal ion will become even more covalent. However, it is also seen that the oxygen O(1s) signals of the more ionic species will be shifted more toward lower energies, than the more covalent toward higher energies (which almost do not change BE in presented in this paper case). Actually, if we would treat the oxygen O(1s) as one singular peak in the case of our perovskite crystals, then the behavior described above by Barr would be true in this case.

Acknowledgment. D.A.P. thanks Dr. Andrzej Wawro from the Institute of Physics, Polish Academy of Science in Warsaw for fruitful discussions.

References and Notes

- (1) Werme, L. O.; Manne, R.; Baer, Y. *ESCA Applied to Free Molecules*; North-Holland: Amsterdam, 1969.

- (2) Siegbahn, K.; Nordling, C.; Fahlman, A.; Nordberg, R.; Hamrin, K.; Hedman, J.; Johansson, G.; Bergmark, T.; Karlsson, S. E.; Lindgren, I.; Lindberg, B. *Nova Acta Regiae Soc. Sci., Ups.* **1967**, *4*, 20.
- (3) Barr, T. L.; Modern ESCA, *The Principles and Practice of X-ray Photoelectron Spectroscopy*, CRC Press: Boca Raton, FL, 1994.
- (4) Barr, T. L. *Appl. Surf. Sci.* **1983**, *15*, 1.
- (5) Barr, T. L.; Lishka, M. A. *J. Am. Chem. Soc.* **1986**, *108*, 3178.
- (6) Barr, T. L. *Zeolites* **1990**, *10*, 760.
- (7) He, H.; Alberti, K.; Barr, T. L.; Klinowski, J. *Nature* **1993**, *365*, 429.
- (8) Grünert, W.; Muhler, M.; Schröder, K.-P.; Sauer, J.; Schlögl, R. *J. Phys. Chem.* **1994**, *98*, 10920.
- (9) Shyu, J. Z.; Skopinski, E. T. Goodwin, J. G.; Sayari, A. *Appl. Surf. Sci.* **1985**, *21*, 297.
- (10) Pawlak, D. A.; Wozniak, K.; Frukacz, Z.; Barr, T. L.; Fiorentino, D.; Seal S. *J. Phys. Chem. B* **1999**, *103*, 1454.
- (11) Sobczak, E.; Zymierska, D.; Ebel, H. *Acta Phys. Pol. A* **1996**, *89*, 329.
- (12) Pawlak, D. A.; Wozniak, K.; Frukacz, Z.; Barr, T. L.; Fiorentino, D.; Hardcastle S. *J. Phys. Chem. B* **1999**, *103*, 3332.
- (13) Czocharalski, J. *Z. Phys. Chem.* **1918**, *92*, 219.
- (14) Ito, M.; Pawlak, D. A.; Shimamura, K.; Fukuda, T.; Wakahara, A.; Yoshida, A.; Seki, Y.; Oda, O. *J. Cryst. Growth* **2001**, article in press.
- (15) Cumpson, P. J.; Seah, M. P. *Surf. Interface Anal.* **1992**, *18*, 345.
- (16) Pawlak, D. A.; Ito, M.; Oku, M.; Shimamura, K.; Fukuda, T. Manuscript in preparation.
- (17) Pawlak, D. A.; Ito, M.; Dobrzycki, L.; Wozniak, K.; Oku, M.; Shimamura, K.; Fukuda, T. *J. Phys. Chem. B* manuscript in preparation.
- (18) Klinowski, J.; Barr, T. L. *Acc. Chem. Res.* **1999**, *32*, 633–640.
- (19) Iwakuro, H.; Tatsuyama, C.; Ichimura, S. *Jpn. J. Appl. Phys.* **1982**, *21*, 94.
- (20) Sarma, D. D.; Rao, C. N. R. *J. Electron. Spectrosc. Relat. Phenom.* **1980**, *20*, 25.
- (21) Gomes, H. A. B.; Bulhoses, L. O. de S.; de Castro, S. C.; Damiao, A. J. *J. Electrochem. Soc.* **1990**, *137*, 3067.
- (22) Nefedov, V. I.; Firsov, M. N.; Shaplygin, I. S. *J. Electron. Spectrosc. Relat. Phenom.* **1982**, *26*, 65.
- (23) Vasquez, R. A. *J. Electron. Spectrosc. Relat. Phenom.* **1991**, *56*, 217.
- (24) Van Doveren, H.; Verhoeven, J. A. Th. *J. Electron. Spectrosc. Relat. Phenom.* **1980**, *21*, 265.
- (25) Uwamino, Y.; Ishizuka, Y.; Yamatera, H. *J. Electron. Spectrosc. Relat. Phenom.* **1984**, *34*, 69.
- (26) Howng, W. Y.; Thorn, R. J. *J. Chem. Phys. Solids* **1980**, *41*, 75.